Study of Anion Adsorption at the Gold–Aqueous Solution Interface by Atomic Force Microscopy

S. Biggs,† P. Mulvaney,† C. F. Zukoski,‡ and F. Grieser*,†

Contribution from The Advanced Mineral Products Research Centre, School of Chemistry, University of Melbourne, Parkville, Victoria 3052, Australia, and School of Chemical Engineering, University of Illinois, Urbana, Illinois 61801

Received March 25, 1994®

Abstract: The forces between a gold coated colloidal silica sphere and a pure gold plate have been measured in aqueous solution as a function of electrolyte concentration using an atomic force microscope (AFM). Forces in the presence of gold(III) chloride ($HAuCl_4$), sodium chloride, and trisodium citrate were recorded as a function of concentration. Each of these anion species is present during the formation of colloidal gold by the reduction of gold(III) chloride with trisodium citrate. In pure water the force between the gold surfaces was exclusively attractive. In sodium chloride or trisodium citrate solution a repulsive interaction was observed which is attributed to the adsorption of these anions at the gold/water interface. The observed interaction force in gold(III) chloride solution was always attractive, the surface potential never exceeding 20 mV. Data taken in aqueous solutions of citrate and chloride ions together suggested that the citrate ions were preferentially adsorbed to the surface of the gold. Addition of gold(III) chloride to the AFM liquid cell after the pre-adsorption of citrate anions caused the force of interaction to change from a repulsive force to an attractive one initially as the gold(III) chloride was reduced to gold by the citrate anions. After a few minutes the repulsive interaction between the surfaces reappeared as the gold(III) chloride was exhausted. Careful analysis of the short range (<10 nm) forces present for all of the above systems suggests that short range repulsive forces are important in determining the stability of gold colloids. Finally, the surface potentials obtained from the AFM data are compared to literature values obtained by electrophoresis for gold colloids prepared by citrate reduction and the role of each of the anions in determining gold colloid stability is assessed.

Introduction

Faraday's gold sol,[1] prepared by the reduction of gold(III) chloride with citrate anions, in aqueous solution, is one of the earliest and most well-documented examples of the preparation of a stable colloid in the laboratory. The stability of these sols over long periods is due to the development of charge at the gold–aqueous solution interface by anion adsorption, which confers electrostatic stability of the system.[2] Despite the fact that stable sols of gold were prepared in this pioneering work over a century ago, the role of each of the anions in determining the stability of both the nascent and final gold particles has not been clearly established.

The majority of studies on gold sols have been concerned mostly with their coagulation behavior or their optical properties and have not considered the origin of the surface charge.[3,4] The reduction of gold(III) chloride with citrate leads to the formation of gold and the liberation of chloride anions. At any time, therefore, during the reduction there will be at least four different anions present in the reaction medium: gold(III) chloride ($AuCl_4^-$); citrate; chloride; and hydroxide anions. Evidence for the adsorption of each of these species at the gold–aqueous interface has been obtained from a wide variety of chemical techniques. However, it is as yet unclear which of these anions confers stability on the colloids both during and after nucleation.

The affinity of halide ions for the gold–aqueous interface is indicated by the high stability constants for gold–halide complexes.[5] Experimentally, halide adsorption has been well established through electrochemical studies.[6] Other electrochemical studies using ellipsometry,[7] specular reflectance,[8] and radiotracer techniques[9] have also been employed leading to the proposal that hydroxide ions are specifically adsorbed at the gold–water interface.[10] It is also well-known that the surface potential of the pure gold surface, from electrokinetic measurements, becomes more negative with increasing pH.[11]

It is commonly accepted that the surface electrical charge of colloidal gold formed by citrate reduction is generated from the adsorption of the reducing agent at the interface.[11] In a series of studies on the nucleation and coagulation of colloidal gold, Turkevich and co-workers[12–14] demonstrated that the stability of the colloid was determined by the changes in surface potential due to the adsorption of citrate anions in the presence of a non-adsorbing background electrolyte. Direct evidence for the presence of citrate ions at the particle surface has been obtained from surface enhanced Raman spectroscopy.[15]

An interesting observation during the reduction process of $AuCl_4^-$ by citrate at moderate temperatures (60–80 °C) is that the sol appears bluish-purple in the early stages of the reaction before becoming pinkish-red as the reaction proceeds toward completion. Turkevich and co-workers[14] showed that an increased size or aggregation would lead to a bluer color while increased polydispersity in shape led to a deeper red color. They found no

* Author to whom correspondence should be addressed.
† University of Melbourne.
‡ University of Illinois.
® Abstract published in *Advance ACS Abstracts*, September 1, 1994.

(1) Faraday, M. *Phil. Trans.* **1857**, *147*, 145.
(2) Coehn, A.; Schafmeister, O. Z. *Phys. Chem.* **1927**, *125*, 401.
(3) Blatchford, C. G.; Campbell, J. R.; Creighton, J. A. *Surf. Sci.* **1982**, *120*, 435.
(4) Quinten, M.; Kreibig, U. *Surf. Sci.* **1986**, *172*, 557.
(5) Finkelstein, N. P.; Hancock, R. D. *Gold Bull.* **1974**, *7*, 72.
(6) Lingane, J. J. *J. Electroanal. Chem.* **1962**, *4*, 332.
(7) Paik, W-K.; Genshaw, M. A.; Bockris, J. O'M. *J. Phys. Chem.* **1970**, *74*, 4266.
(8) Anderson, W. J.; Hansen, W. N. *J. Electroanal. Chem.* **1973**, *47*, 229.
(9) Horanyi, G.; Rizmayer, E. M. *J. Electroanal. Chem.* **1983**, *152*, 211.
(10) Kirk, D. W.; Foulkes, F. R.; Graydon, W. F. *J. Electroanal. Soc.* **1980**, *127*, 1069.
(11) Thompson, D. W.; Collins, I. R. *J. Colloid Interface Sci.* **1992**, *152*, 197.
(12) Turkevich, J.; Stevenson, P. S.; Hillier, J. *Discuss. Faraday Soc.* **1951**, *11*, 58.
(13) Turkevich, J.; Garton, G.; Stevenson, P. C. *J. Colloid Sci.* **1954**, *9*, 26.
(14) Enüstün, B. V.; Turkevich, J. *J. Am. Chem. Soc.* **1963**, *85*, 3317.
(15) Sandroff, C. J.; Herschbach, D. R. *Langmuir* **1985**, *1*, 131.

0002-7863/94/1516-9150$04.50/0

evidence for the adsorption of anions affecting the color of the sol. Electron micrographs[16] of the sol taken at various times during the reduction process showed particle aggregates of around 200–300 nm diameter initially, while at the end of the reaction individual 10 nm particles were exclusively observed. In an earlier communication from this laboratory[17] we presented initial data on the interaction forces for gold surfaces in the presence of either citrate, $AuCl_4^-$, or mixtures of these anions measured using an atomic force microscope (AFM). These data suggested that the $AuCl_4^-$ was preferentially bound to the gold surface and that as it was progressively reduced it was replaced at the surface by the abundant citrate ions. The initial adsorption of the gold(III) chloride led to a low charge density at the surface and hence transient, weak flocculation. As the citrate was adsorbed, the charge at the surface rose, leading to peptization of the sol. In this paper we present a full study of the role of all the anions present in determining the stability of gold sols both during and after their preparation.

Experimental Section

Materials. (a) Reagents. All water was distilled and subsequently purified to Millipore Milli-Q quality. Gold(III) chloride ($HAuCl_4$), trisodium citrate, sodium chloride, sodium hydroxide, and hydrochloric acid were of analytical grade and were not purified further before use.

(b) Gold Probes. Two types of gold probe were prepared for use in these studies. One type of probe was based upon using the commercially available silicon nitride cantilevers with pyramidal tips (Digital Instruments). The second was prepared by attaching a colloidal sphere of silica to one of the commercial cantilevers with a small amount of resin (Shell Epikote 1002) according to the technique of Ducker et al.[18] Typically the spheres used had radii of between 3 and 6 μm.

In both cases the probes were coated by sputter deposition of gold. The surfaces were typically coated for 3 min. Analysis of the film thickness by AFM imaging at the edge of a film of gold deposited on mica suggested that the thickness of the deposited gold film was of the order of 0.3 μm.

(c) Polished Gold Plate. AFM measurements were made against a plate of 24 carat gold (purity 99.999%) polished to optical smoothness. The mean roughness of this plate, determined from an AFM image, recorded using a commercial silicon nitride cantilever, was found to be ± 2 nm across an area of 1 μm $\times$ 1 μm. This plate was cleaned by soaking in chromic acid for 15 min before rinsing in copious quantities of pure water.

Force Measurements with the AFM. The use of an AFM for surface force measurements has been described previously by a number of other authors[18,19] and will only be summarized here.

Force–distance information was obtained from a Nanoscope III AFM (Digital Instruments) which was operated in the "force mode". In this operating mode the X–Y raster motion of the sample on the scanning piezo electric crystal is suspended and the sample is moved toward and away from the cantilever in the Z direction by the application of a saw tooth voltage.

In a typical experiment, one of the colloid probes was mounted into the commercially available liquid cells (Digital Instruments) and was washed with ethanol before drying with a steady stream of nitrogen. At this stage, the clean gold plate which was still submerged under water was rapidly dried by rinsing with ethanol and drying under a stream of nitrogen. It was then mounted immediately onto the AFM-D piezo scanner, and the liquid cell, mounted into the head unit, was rapidly attached to the scanner. The probe was then brought into close proximity with the surface. At this point, the solution for study was pumped into the liquid cell from a sealed bulk reservoir using a peristaltic pump. It was important to perform each of these steps rapidly in order to minimize the contact time of the gold surface with the atmosphere and hence keep the contamination by organic impurities to a minimum. Clean surfaces were seen to wet completely with water without the presence of any air bubbles in the cell.

All solutions used here were bubbled with N_2 gas for 30–60 min prior to use and continuously thereafter for the duration of each experiment. The pH was monitored in situ and 30 min were allowed after each addition of acid or base for the attainment of equilibrium. After any change in salt concentration 30 min were allowed under constant circulation for the surfaces to come to equilibrium.

The deflection of the cantilever bearing the colloid probe is monitored by the changes in voltage from a split photodiode onto which is focused a laser beam that is reflected from the rear of the cantilever. The software of the AFM generates a file that contains the output of the photodiode and the displacement of the sample on the piezo crystal. These raw data were then converted into real force versus separation data following the principle of Ducker et al.[18] which requires the definition of a position of zero force and a position of zero separation. Zero force is simply defined as the photodiode voltage at large separations where a change in the crystal position has no effect on the cantilever deflection. Zero separation is defined as being when the change in crystal position causes an equal change in the cantilever displacement, the so-called region of constant compliance. From a knowledge of these two positions and the slope of the region of linearity at constant compliance, the force as a function of separation can be calculated.

In the majority of previous direct force interaction studies on colloid systems the only unknown factor has been the spring constant, with the manufacturers quoted values being used. For this work, the spring constants were experimentally determined by measuring the frequency of oscillation of the cantilever when spheres of known mass were attached to it following the procedure of Hansma et al.[20] Using this technique, the 100 μm long thick legged cantilevers were found to have a spring constant of 0.32 ± 0.01 N/m.

Results and Discussion

For the sake of clarity the experimental results are presented as follows. In sections I–IV we examine the adsorption of each of the anions onto gold surfaces under conditions similar to those found during the preparation of gold sols. We show that citrate ion is the important stabilizing species at the gold–water interface. In section V, we then present the results of experiments where we have attempted to monitor *in situ* the changes in the surface potential of gold surfaces as the reduction of gold chloride by citrate ions is taking place. Finally, in sections VI and VII we discuss the contribution of short range forces to the stability of gold sols and the relevance of the AFM data to earlier work on gold sols.

I. Gold–Gold Interactions in Water. The cleanliness of the surfaces was routinely verified before each experiment by recording the attractive van der Waals interaction between the gold surfaces in pure water at a pH of around 6.3. A full discussion of the determination of the van der Waals curve for this interaction has been given elsewhere[21] and will not be presented here. If a van der Waals curve for gold–gold interactions across water could not be obtained prior to each experiment, the surfaces were recleaned in chromic acid before continuing.

II. Gold Interactions with Chloride Ions. The surface potential of the gold as a function of chloride concentration was determined from the force–distance information for a spherical gold probe against the polished gold surface at any given chloride concentration and at a constant pH of 6.3. Typical data curves for the log of the normalized force (F/R) against separation distance for the approach of the two gold surfaces at chloride concentrations of 2×10^{-6}, 2×10^{-5}, and 4×10^{-5} M are shown in Figure 1. The best fits to the experimental data were calculated by using the nonlinearized Poisson–Boltzmann equation with both constant surface charge and constant surface potential boundary conditions using the technique of Chan et al.[22] The full, retarded, van der Waals force was then added to the electrostatic component to obtain the force of interaction–distance curves. At the chloride

(16) Chow, M. K.; Zukoski, C. F. *J. Colloid Interface Sci.* **1994**, *165*, 97.
(17) Biggs, S.; Chow, M. K.; Zukoski, C. F.; Grieser, F. *J. Colloid Interface Sci.* **1993**, *160*, 511.
(18) Ducker, W. A.; Senden, T. J.; Pashley, R. M. *Langmuir* **1993**, *9*, 2232.
(19) Israelachvili, J. N. *Intermolecular and Surface Forces*, 2nd ed.; Academic Press: San Diego, 1992.
(20) Cleveland, J. P.; Manne, S.; Bocek, D.; Hansma, P. K. *Rev. Sci. Instrum.* **1993**, *64*, 403.
(21) Biggs, S.; Mulvaney, P. *J. Chem. Phys.* **1994**, *100*, 8501.
(22) Chan, D. Y. C.; Pashley, R. M.; White, L. R. *J. Colloid Interface Sci.* **1980**, *77*, 283.

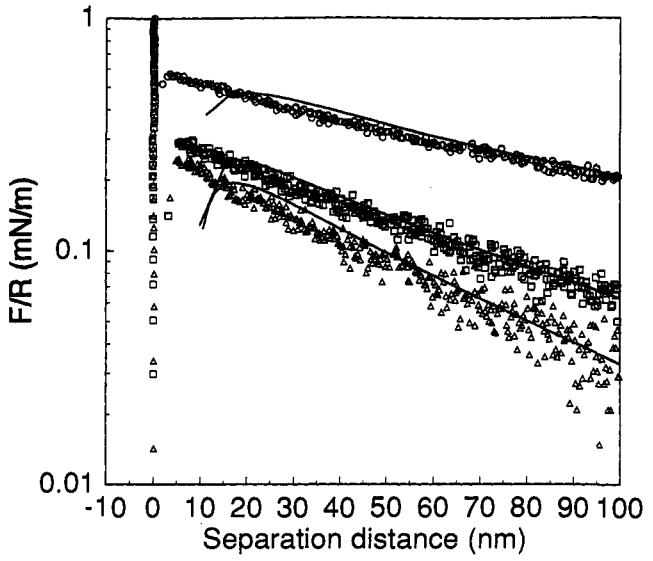

Figure 1. The forces observed between a gold sphere and a gold plate in aqueous sodium chloride solution at three concentrations ($T = 20$ °C): (○) 2×10^{-6} M; (□) 2×10^{-5} M; (△) 4×10^{-5} M. The data were fitted to the nonlinear Poisson–Boltzmann equation assuming constant surface charge with the following values for the Debye length, κ^{-1}, and surface potential, ψ_s: 2×10^{-6} M, $\kappa^{-1} = 175.5$ nm, $\psi_s = 110$ mV; 2×10^{-5} M, $\kappa^{-1} = 68$ nm, $\psi_s = 50$ mV; 4×10^{-5} M, $\kappa^{-1} = 48.1$, $\psi_s = 40$ mV. Solution pH = 6.3.

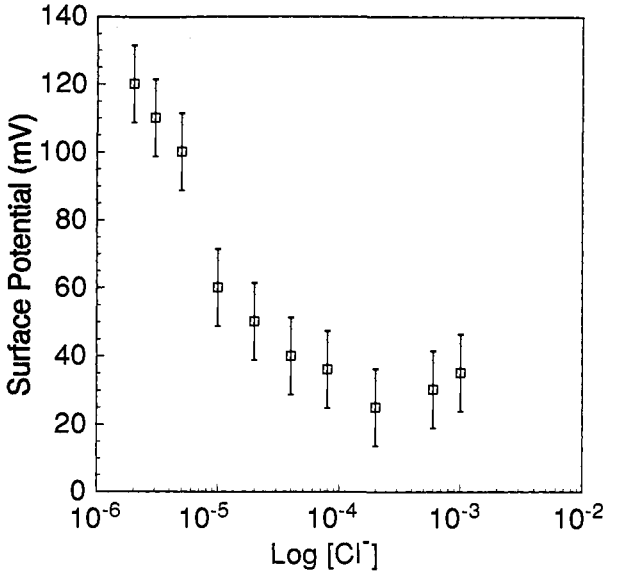

Figure 2. Variation of the fitted surface potential at infinite separation as a function of chloride ion concentration determined from the experimental force–distance interaction data. Solution pH = 6.3.

concentrations shown, the force is repulsive over the entire separation distance. At small separations (<20 nm), where the large van der Waals attractive contribution to the overall force profile might be expected to dominate, a short range repulsive barrier is seen. This repulsion was observed for all the concentrations of chloride examined in this study. The only reported data for the interaction of gold surfaces in the presence of chloride ions[18] studied by AFM also showed this extra repulsive barrier inside the expected jump-in distance. The authors were unable to fit their observed data, for a 3.5 μm sphere which showed a jump-in distance of 3 nm, with DLVO theory. They proposed that this was probably due to either hydrophobic material adsorbed on the gold surfaces or problems in defining the plane of charge. However, in the absence of chloride ions we found no evidence for surface contamination. The origin and extent of this force will be discussed more fully in section VI.

At chloride concentrations of less than 1×10^{-5} M the experimentally observed data were fitted to a theoretically calculated value of the Debye length, κ^{-1}, based upon the total ion concentration in solution. Briefly, at any concentration κ^{-1} is fixed (to the appropriate value) and the baseline of the raw data is then adjusted until the decay length of the data is equivalent to this value. At this point the best fit to the potential for these data is obtained. This procedure was adopted because the errors in determining the position of the baseline are high for large values of the decay length. At concentrations of 1×10^{-5} M chloride and above, the determination of zero force was more easily reproducible. For the force–separation data presented in Figure 1, the Debye length and the diffuse layer potential both decrease as the salt concentration is increased. The variation in the potential as a function of the chloride concentration, at a pH of 6.3, is shown in Figure 2.

At all concentrations of chloride ion, the experimentally obtained data were fitted more closely by an interaction at constant charge. The implication of this is that the adsorbed chloride ion concentration remains essentially constant as the surfaces approach each other, the adsorption free energy being high enough to prevent any ion desorption.

All the force profiles seen were very similar to those reported previously for mineral oxide systems.[18,23] As is typical for AFM studies of interaction forces, only the data for the approach of the surfaces were used in the calculation of the surface potentials. The adherence data obtained during the separation of the surfaces showed the large fluctuations in absolute values observed previously, which have been attributed to rolling and bending of the cantilever.[18]

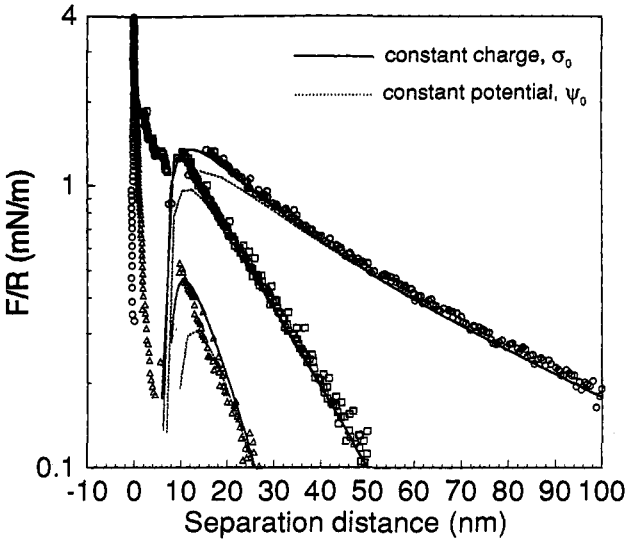

Figure 3. The forces observed between a gold sphere and a gold plate in aqueous trisodium citrate solutions at three concentrations ($T = 20$ °C); (○) 6×10^{-6} M; (□) 1×10^{-4} M; (△) 3×10^{-4} M. The data were fitted to the nonlinear Poisson–Boltzmann equation assuming constant surface charge with the following values for the Debye length, κ^{-1}, and surface potential, ψ_s: 6×10^{-6} M, $\kappa^{-1} = 58.8$ nm, $\psi_s = 125$ mV; 1×10^{-4} M, $\kappa^{-1} = 15.3$ nm, $\psi_s = 84$ mV; 3×10^{-4} M, $\kappa^{-1} = 8.9$ nm, $\psi_s = 53$ mV. Solution pH = 6.3.

III. Gold Interactions with Trisodium Citrate. In Figure 3 we present data for the interaction of the two gold surfaces in the presence of three concentrations of citrate. Again we see that the Debye length and the diffuse layer potential decrease with increasing salt concentration at a constant pH of about 6.3. The experimentally determined decay lengths were again seen to be well fitted by theoretical values. As in the case of chloride adsorption, the observed potentials decreased with increasing salt concentration from the lowest concentration examined.

(23) Larson, I.; Drummond, C. J.; Chan, D. Y. C.; Grieser, F. *J. Am. Chem. Soc.* **1993**, *115*, 11885.

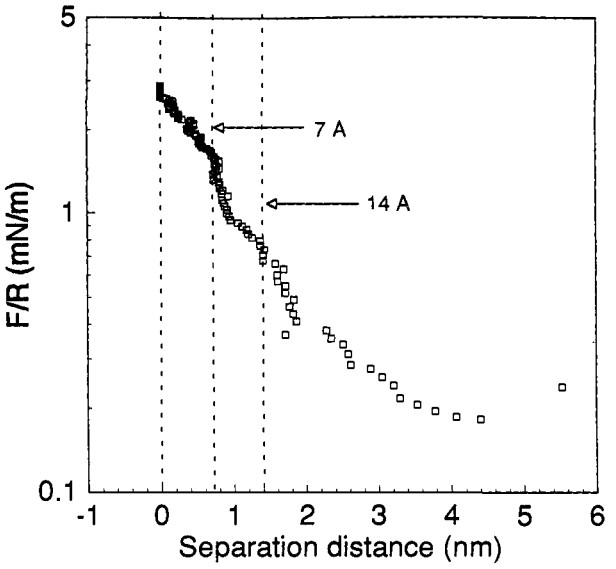

Figure 4. The short range forces between a gold sphere and a gold plate in 1×10^{-4} M aqueous trisodium citrate solution. Hard-wall-type barriers are indicated at 7 Å and 14 Å separation.

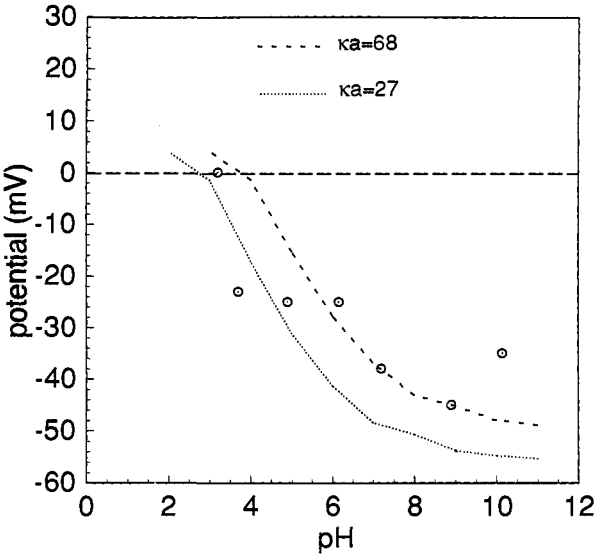

Figure 5. Experimentally determined surface potentials as a function of pH for a gold sphere and a gold plate in 1×10^{-3} M sodium chloride/1×10^{-4} M trisodium citrate aqueous solution. The potentials were determined from the best fits to the nonlinear Poisson–Boltzmann equation with constant surface charge and constant surface potential as boundary conditions using a Debye length, κ^{-1}, of 5.3 nm. The data are compared to ζ potentials for gold colloids under the same solution conditions determined from the mobility data of Thompson and Collins[11] using κa = 27 and 68, corresponding to an average particle size of between 0.2 and 0.5 μm. The mobilities were converted to potentials using the algorithm of O'Brien and White.[32]

The trivalent molecule citric acid has the following thermodynamic dissociation constants: $K_1 = 1.2 \times 10^{-3}$, $K_2 = 4.9 \times 10^{-5}$, and $K_3 = 2.5 \times 10^{-6}$. Calculations of the species distributions as a function of solution pH using these dissociation constants shows that at pH = 6.3 the predominant species will be the X^{3-} and HX^{2-} anions present at a ratio of about 3:1.

The form of the observed data at small separations varied from that seen for the chloride adsorption where, at all concentrations, repulsive forces were seen to extend beyond the theoretically calculated position for the onset of the potential energy minimum. In addition, the contact of the surfaces at constant compliance was seen to be a "hard" interaction with a single gradient. In the case of citrate adsorption the form of the data at small separations was found to be dependent upon the salt concentration. At all citrate concentrations the colloid probe was consistently seen to jump toward contact from around 10 nm separation. This jump-in distance compares very well with the distance of 9 nm determined in pure water where only attractive forces were operating.[21] At citrate concentrations below 1×10^{-5} M the surfaces were always observed to jump into a hard wall contact. However, at higher concentrations some form of steric repulsive barrier was seen from separations of 5–7 nm into zero separation. It is worth noting that in all cases the raw data ultimately showed a region of constant compliance which could not be "pushed through" by increasing the load on the surfaces. Before these regions of constant compliance, the raw data for the surfaces in contact showed a varying response of the photodiode with increasing load on the surfaces and periodic short steps characteristic of the "squeezing out" of ions or other adsorbed species from between the surfaces.[24] It should be noted that when in contact the effects of surface roughness on the observed force interactions will be at their greatest. Since we have no measure of the local radii of curvature for the interacting parts of the two surfaces, the measured surface energies are totally unreliable in this contact zone. However, the form of the interactions and the distances measured should be unaffected by the different sizes of the contacting regions. Thus, these contact regions will not be discussed with reference to their relative energy magnitudes but rather by comparing the form of these interactions and the distances over which they operate.

An example of these data at short separations is shown in Figure 4. A close examination reveals two interesting features. At all concentrations examined here, two repulsive hard-wall-type steps of about 7 Å in size were seen immediately prior to the attainment of zero separation. The appearance and size of these steps were consistant at all citrate concentrations examined here. Outside of these steps, the repulsive barrier as the surfaces were squeezed together was seen to be variable in appearance. Again, a full discussion of these short range interactions will be presented in section VI.

The theoretically determined best fits to the experimental data shown in Figure 3, at constant charge and constant potential, were calculated by assuming a 7 Å ion barrier on each surface corresponding to an adsorbed layer of citrate ions.[25] The combined electrostatic repulsion and van der Waals attraction curves were then calculated by determining the full retarded attractive interaction from the experimental zero of separation and adding this to the electrostatic repulsion located at 14 Å outside this plane. At all concentrations this leads to an excellent agreement between the theoretical fits and the experimental data, the jump-in distance of around 10 nm correlating well with theoretical predictions.

IV. Gold Interactions in the Presence of Both Citrate and Chloride Ions. The influence of pH on the interaction potentials for gold surfaces in the presence of 1×10^{-4} M citrate and 1×10^{-3} M chloride ions is shown in Figure 5. These concentrations were selected for study because they represent the typical expected salt concentrations for a gold colloid formed from the citrate reduction of gold(III) chloride at the end of the reaction. These data are plotted together with electrokinetic potentials calculated from the published mobility data of Thompson and Collins[11] obtained under identical conditions. Two potential–pH curves were derived from their published mobility data by using the upper and lower particle sizes of the polydisperse gold dispersion they employed. The size limits used were 0.2 to 0.5 μm which gave κa limiting values of 27 and 68 for the mobility to potential conversion. Clearly there is good agreement between these data, determined independently and with different techniques. It has

(24) Drummond, C. J. Personal communication.

(25) Leong, Y. K.; Boger, D. V.; Scales, P. J.; Healy, T. W.; Buscall, R. *J. Chem. Soc., Chem. Commun.* **1993**, 640.

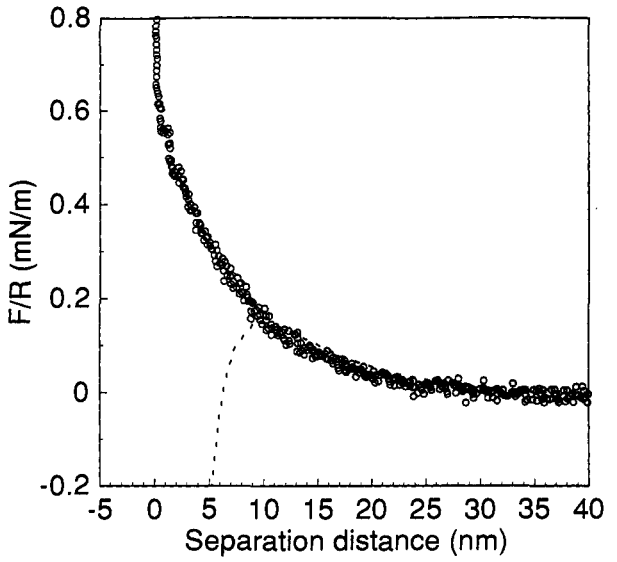

Figure 6. The forces observed between a gold sphere and a gold plate in 1×10^{-3} M sodium chloride/1×10^{-4} M trisodium citrate aqueous solution at pH = 8.9. The data were fitted to the nonlinear Poisson–Boltzmann equation assuming constant surface charge with a Debye length, κ^{-1}, of 5.3 nm and a surface potential, ψ_s, of 45 mV.

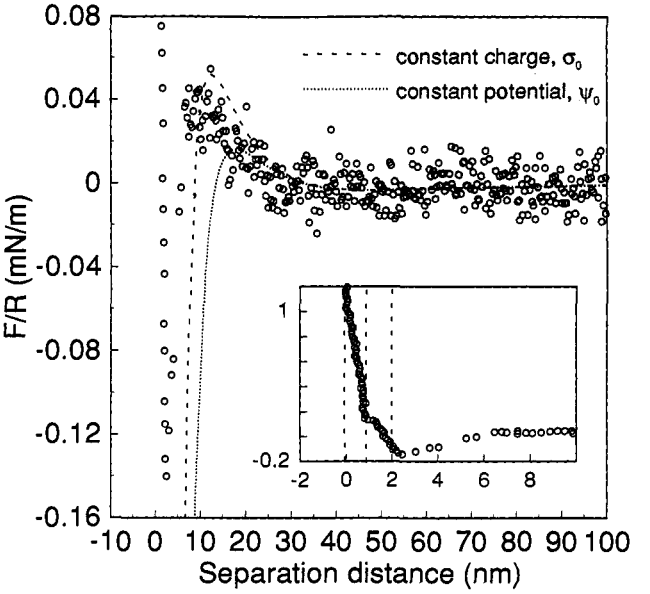

Figure 7. The forces observed between a gold sphere and a gold plate in 1×10^{-1} M sodium chloride/1×10^{-4} M trisodium citrate aqueous solution at pH = 3.7. The data were fitted to the nonlinear Poisson–Boltzmann equation assuming constant surface charge and constant surface potential as the upper and lower boundary conditions and with a Debye length, κ^{-1}, of 5.3 nm and a surface potential, ψ_s, of 23 mV. A 20 Å offset between the effective plane of charge due to the adsorbed citrate anions and the attractive van der Waals interaction between gold surfaces was employed (see text for details). Inset shows the data at small separations; the two 10 Å barriers may be clearly seen.

been previously demonstrated for the interaction of TiO_2 surfaces in KNO_3 that the potential determined from electrophoretic mobilities correlates closely with that calculated from AFM measurements.[23] These data for the gold–gold interactions support this finding.

The potential data presented here offer no direct indication of whether chloride or citrate is preferentially adsorbed at the gold–water interface. Thompson and Collins[11] have examined the effect of adding different concentrations of sodium chloride to gold particles in the presence of a fixed amount of citrate. Their data showed that the added chloride had no effect on the observed mobility of the gold particles. They attributed this to the preferential adsorption of citrate at the gold–water interface. We can obtain indirect evidence for the adsorption of citrate in preference to chloride ions from the experimental force distance profiles.

Curves of the normalized force as a function of surface separation are given in Figures 6 and 7 for pH 8.9 and 3.7, respectively. The data at pH 8.9 (Figure 6) show a continuously repulsive interaction into zero separation. Once again, as for the citrate data (Figure 3), the full theoretical interaction curve was calculated by assuming an offset of 14 Å between the attractive and repulsive parts of the curve. Despite this offset, the theory suggests the rapid onset of a minimum at about 10 nm separation which should be evidenced experimentally by a jump into contact. It is clear that such a jump is not present but, rather, we see a continuous repulsion into around 14 Å where we may identify a steric barrier due to adsorbed citrate ions. Expanding this region of short range repulsion, Figure 8, we see that there are two regions. The first extends from about 80 Å in to 14 Å, where there is a clear break in the data, followed by a second repulsive regime into zero separation which has a small barrier at 7 Å distance. A closer examination of the region from 80 to 20 Å suggested the possibility of some periodic ordering with 5 Å wide barriers separated by 2.5 Å gaps. While the barriers at 7 ± 2 and 14 ± 2 Å were consistent and reproducible at this pH, the exact form of the data between 20 and 80 Å was not determined due to inconsistencies in the data between different samples.

Data for this system at a pH of 3.7 (Figure 7) show two 10 ± 2 Å hard-wall barriers before constant compliance, at zero separation, is achieved. However, there is no further short range repulsive barrier inside the calculated potential minimum. By using a 20 Å offset, taken from Figure 7, for the combined

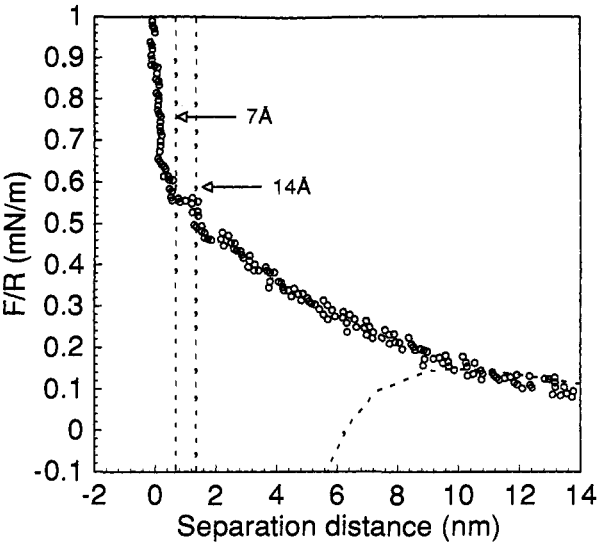

Figure 8. Enlarged scale of the force data presented in Figure 6 showing the short range interactions. Hard-wall barriers at 7 and 14 Å are indicated.

attractive and repulsive theoretical fits, the point at which the surfaces jump together is well fitted. The theoretical fit at 23 mV predicts the presence of a secondary minimum at about 30 nm separation. The scatter of the experimental data prevents an unequivocal demonstration of this minimum. However, the data generally decreased from the baseline zero between 50 and 25 nm separation before passing through the observed maximum.

V. Gold Interactions with Gold Chloride and Gold Chloride/Citrate. A typical force–distance curve for gold–gold in the presence of $HAuCl_4$ at concentrations between 1 μM and 1 mM and at a pH of about 6 is shown in Figure 9. At all concentrations, it was observed that the interaction was attractive, the maximum diffuse layer potential attained being about 20 mV. Thus gold-

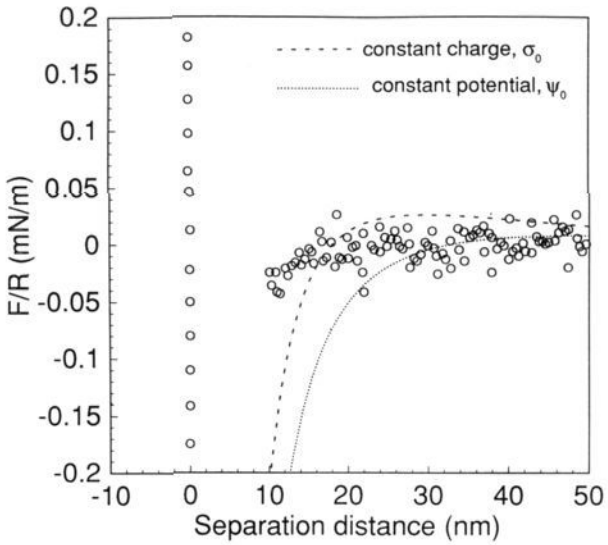

Figure 9. The forces observed between a gold sphere and a gold plate in 1×10^{-4} M $HAuCl_4$ aqueous solution. The data were fitted to the nonliniear Poisson–Boltzmann equation assuming constant surface charge and constant surface potential as the upper and lower boundary conditions and with a Debye length, κ^{-1}, of 30 nm and a surface potential, ψ_s, of 23 mV. Solution pH = 6.0.

(III) chloride cannot be responsible for the electrostatic stabilization of the nascent gold nuclei formed during the reduction process.

The question which then arises is, which species determines the state of the surface during the actual nucleation and growth of the sols? When both $AuCl_4^-$ and citrate ions are present in the solution, either anion may be "potential determining". To address this question we therefore monitored the gold–gold forces during the nucleation process as follows. Citrate ion at 1 mM was equilibrated with the gold surfaces for 30 min. A repulsive interaction (Figure 10a) was observed. A mixture of 1 mM sodium citrate and 0.1 mM gold(III) chloride was then injected into the AFM reaction cell. The mixing time was some 1–5 s. The repulsive interaction disappeared immediately, and an attractive curve similar to that observed for gold chloride alone was observed (Figure 10b). Note that the interaction is weaker than the pure van der Waals interaction, and that the potential well is very shallow. There is also evidence for a push-through due to an adsorbed species on the surface. At low gold chloride concentrations (10 μM), the reemergence of a repulsive interaction was observed after several minutes, while at 0.1 mM $AuCl_4^-$, the interaction remained attractive indefinitely due to the relatively slow kinetics of Au(III) reduction in the AFM cell. We conclude that during $AuCl_4^-$ reduction at a metal gold surface there is only a weak electrostatic barrier present (<20 mV). The steady state surface concentration of citrate ions is small, and there is no evidence for short range repulsive interactions.

As the reaction continued, the photodiode voltage decreased due to an increase in scatter of the beam reflected from the back of the cantilever. This scatter is attributed to the formation of gold colloids on the cantilever. AFM imaging of a surface covered in these colloids shows the surface to be rough. It should be noted that the back of the cantilevers are gold coated. The presence of this gold catalyzes the oxidation of $AuCl_4^-$ by citrate ions, a reaction that is normally slow at room temperatures. This catalysis has been confirmed using seed gold particles in solutions containing $AuCl_4^-$ and citrate.[26] The reaction could therefore only be monitored for about half an hour. In Figure 11, a gold encrusted cantilever is shown after reduction is complete.

These "kinetic" AFM results support the previous finding[17] that the addition of gold chloride to a citrate stabilized gold sol

(26) Unpublished data.

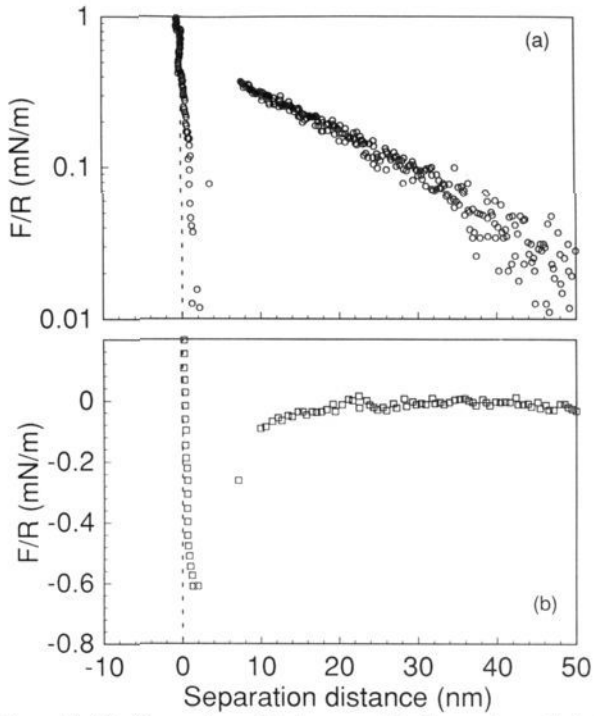

Figure 10. The forces observed between a gold sphere and a gold plate in two different solutions: (a) aqueous 1×10^{-3} M trisodium citrate; (b) immediately after the addition of 1×10^{-4} M $HAuCl_4$ to the system shown in part a, while maintaining the trisodium citrate concentration at 1×10^{-3} M. Note that in both cases the presence of a short range barrier extending 10–20 Å from the experimentally determined point of surface contact. Solution pH = 6.0.

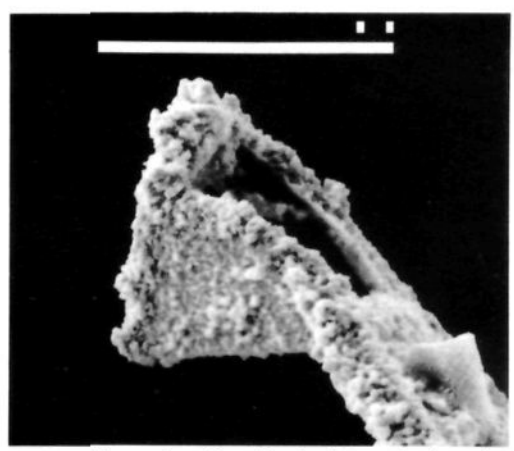

Figure 11. A gold coated cantilver tip after immersion in a solution of $HAuCl_4$ and trisodium citrate at room temperature. The rough surface morphology is due entirely to the catalyzed formation of gold at the gold/water interface via the reduction of the gold(III) chloride by the citrate.

leads to the formation of a blue dispersion of transient aggregates. After several hours, the added gold chloride is completely reduced, and the particles then spontaneously repeptize to give the original pink colored sol, typical of unaggregated particles.

It is worth noting that the transient aggregation that occurs during particle growth is not due to the presence of a secondary minimum (cf. Figure 7). If the gold chloride consumed just a small fraction of the surface citrate ions and caused a corresponding decrease in the surface potential, a secondary minimum may appear, but this would be at surface separations of about 30 nm. There is no evidence for this. The surface citrate appears to be almost completely discharged by the addition of $AuCl_4^-$. The flocculation occurs directly into the primary minimum. Only

when the reduction of $AuCl_4^-$ is near completion does a recharging of the surface permit the full repeptization of the transiently flocculated gold aggregates. It is clear from the force data in Figure 10b, however, that there is some *uncharged* species at the surface which sterically protects the gold particles even as they are growing. If this were not the case, repeptization would be extremely unlikely.

The nature of the adsorbed layer imparting steric stabilization is unknown. It may be that neutral citrate ions are adsorbed, or that an oxidation product of the citrate is present. It is important to mention here that $AuCl_4^-$ hydrolyzes in aqueous solution to form $AuCl_2(OH)_2^-$. At neutral pH's $Au(OH)_3$ is the thermodynamically stable species, and its adsorption onto the gold nuclei would lower the surface potential and provide a stabilizing surface layer. The data presented in Figure 10b do not unfortunately give any information about which of these species, if any, would be favored. All that may be stated is that there is some form of adsorbed steric layer at the surface.

VI. Short Range Force Interactions. For the three systems so far examined, the DLVO[27] theory alone was not adequate to accurately fit the entire data curves. In all cases, extra short range interactions were seen beyond the calculated position for the onset of the potential energy minima in these systems.

The origin and nature of these extra repulsive factors in the interaction force profiles is not obvious. In the case of chloride ion adsorption, the previous data of Ducker et al.[18] also show an extra repulsion beyond the calculated jump-in separation. While these authors attributed this effect to the adsorption of hydrophobic impurities and/or problems with accurate determination of the plane of charge for their system, this does not adequately explain our data. While the effects of adsorbed impurities on gold surfaces must undoubtedly be considered, we have shown in another communication[21] that even in the presence of hydrophobic impurities the strength of the van der Waals interaction for gold–water–gold is such that, at sub-monolayer coverages, it will always determine the extent and form of the attractive interaction. Furthermore, after examining the interactions with chloride ions the system was washed with a continuous flow of water before the citrate ion experiments were performed. The results for adsorbed citrate ions (Figure 3) showed that at low ion concentrations the surfaces jumped together at a separation which was consistent with the calculated retarded Hamaker constant. The presence of any organic hydrophobic impurities on the gold during the chloride studies would be expected to persist and cause similar problems in the citrate experiments. This was not the case, and so we consider the extra repulsion observed in the presence of citrate ions to be a real effect. Furthermore, at low citrate concentrations ($<1 \times 10^{-5}$ M) the whole force curve could be fitted with the DLVO[27] theory, the steric term only becoming important at higher concentrations.

In all cases, the experimentally obtained data were seen to be fitted more closely by theoretical fits to constant charge. Thus, as the surfaces are being brought together, the potential at the surface is constantly increasing. A consequence is that hydrated sodium counterions are attracted into the gap between the surfaces in order to counter balance this potential change. It has been demonstrated previously for mica–mica interactions in aqueous electrolyte that at short separations so-called hydration forces can occur.[28] These forces are attributed to the presence near the negatively charged surface of highly hydrated sodium counterions. As the surface come together, oscillatory forces are observed as layers of water molecules around the sodium ions are "squeezed" out of the gap. Clearly, for this system where large numbers of sodium counterions may be expected between the surfaces, the possibility of comparable interactions must be considered.

It is important to remember that, in the previous studies, for the mica–mica interaction such oscillatory forces were seen to extend over distances of 2–4 nm.[28] In addition they were only seen at higher salt concentrations ($>1 \times 10^{-4}$ M) and in alkaline solutions. In the reported cases here, the short range interactions were seen to extend over greater distances and to be apparent at lower salt concentrations. It is interesting, however, that in the case of the chloride/citrate systems primary minimum was present in acidic media (Figure 7) but absent in alkaline solutions.

In the case of citrate adsorption in the absence of chloride ions, evidence for an oscillatory interaction was not as pronounced. There is clearly, however, a "squeezing" out of adsorbed citrate in the data presented in Figure 4.

The steric barriers seen with the adsorbed citrate ions are more easily understood. When the pH changes from acidic to alkaline conditions the experimentally observed barrier size for the adsorbed citrate ion decreases from 10 ± 2 Å to around 7 ± 2 Å. This may be due to a change in the conformation of the adsorbed species at the interface. In alkaline solution the citrate will be presented predominantly as the X^{3-} anion which will probably adsorb in a rather flat conformation. As the acidity of the solution is increased protonation of the citrate species will occur and the possibility exists that the HX^{2-} and H_2X^- ions extend further into solution than does the X^{3-} anion.

VII. Relevance of Force Data to Gold Colloid Stability. The apparent surface potentials found from the direct force measurements correlate well with the mobility data of Thompson and Collins.[11] They are also in accord with the ζ potential measurements of Turkevich and co-workers,[13] who found potentials of 32–47 mV in 1×10^{-5} M sodium citrate. They are lower than the value obtained by Heard et al.,[29] who used microelectrophoresis to determine the particle mobility. They obtained a value of about 66 mV at an electrolyte concentration of 5×10^{-3} M and at a pH of 5.5. The fact that different techniques yield comparable "surface potentials" demonstrates that the operative potentials in colloid coagulation, force measurements, and electrophoresis are probably very similar and can be considered to be shear plane potentials. A similar result has recently been obtained by Larson et al.,[23] who found that AFM "surface" potentials on TiO_2 corresponded very closely to ζ potentials derived fronm electrophoresis experiments. However to explain the stability of gold sols at such low potentials, Enüstün and Turkevich[14] then had to use a Hamaker constant of 2.3×10^{-20} J. We have recently confirmed[21] by AFM that the unretarded Hamaker constant for gold surfaces in water is 2.5×10^{-19} J, a factor of ten higher than this. Thus, the low potentials and high Hamaker constant are inconsistent with the stability of the sols. However it is clear from the direct force measurements that it is the presence of short range forces in citrate solution that prevents gold colloid coagulation. At neutral pH values and in the presence of citrate ions, the force data show that inside the expected primary minimum, steric forces prevent coagulation. A repulsive interaction is found right up to contact between the surfaces.

The rate at which the surfaces come into contact during the AFM experiment is not much faster than the rate of Brownian encounters in solution. Taking $D \sim 10^{-8}$ cm^2 s^{-1} for 100 Å radius gold particles,[33] the double layer interaction should occur over a time $\tau \sim (1/D\kappa^2) \sim 10^{-2}$ s. The AFM piezo drives the surfaces together at about 2–5 μm s^{-1} so that the 100 Å thick double layer

(27) (a) Derjaguin, B.; Landau, L. *Acta Physiochem.* **1941**, *14*, 633. (b) Verwey, E. G. W.; Overbeek, J. Th. G. *Theory of the Stability of Lyophobic Colloids*; Elsevier: Amsterdam, 1948.

(28) (a) Pashley, R. M. *J. Colloid Interface Sci.* **1981**, *83*, 531. (b) Pashley, R. M. *J. Colloid Interface Sci.* **1981**, *80*, 153. (c) Israelachvili, J. N.; Pashley, R. M. In *Biophysics of Water*; Franks, F., Ed.; Wiley: New York, 1982, pp 183–194.

(29) Heard, S. M.; Grieser, F.; Barraclough, C. G.; Sanders, J. V. *J. Colloid Interface Sci.* **1983**, *93*, 545.

(30) Rabinovich, Ya. I.; Churaev, N. V. *Kolloidn. Zh.* **1990**, *52*, 256.

(31) Parsegian, V. A.; Weiss, G. H. *J. Colloid Interface Sci.* **1981**, *81*, 285.

(32) O'Brien, R. W.; White, L. R. *J. Chem. Soc., Faraday Trans. 2* **1978**, *74*, 1607.

(33) Hunter, R. J. *Foundations of Colloid Science*; Oxford University Press: New York, 1989; Vol. 1.

is traversed in 10^{-3}–10^{-2} s. This steric force is therefore a real barrier that will be experienced by gold colloids during encounters in solution.

Conclusions

The adsorption of either chloride or citrate anions at the gold/water interface leads to the development of sufficient surface charge to cause a repulsive interaction between a gold sphere and a gold plate in aqueous solution. However, when gold(III) chloride anions adsorb at the same interface only an attractive interaction is observed. In this case the maximum surface potential does not exceed 20 mV, a value insufficient to overcome the large attractive van der Waals component to the overall force. When citrate and chloride anions were added together the experimental force profiles observed showed a short range steric barrier equivalent in magnitude to that expected for a layer of citrate anions on each surface, indicating the preferential adsorption of the citrate at the interface.

The repulsive interaction observed in the presence of adsorbed citrate anions was immediately replaced by an attractive interaction upon addition of gold(III) chloride. After complete reduction of gold(III) chloride by citrate a repulsive interaction was once again observed. The presence of an adsorbed species at the interface throughout this reaction was evident from the force data when the surfaces were in contact.

The force–distance profiles obtained in this study demonstrate directly the complexity of the overall forces responsible for the stability of a colloidal material such as gold. In addition to electrostatic repulsive forces other, unexplained short range repulsions are present at the gold/water interface in the presence of adsorbed anions.

Acknowledgment. We are indebted to Dr. Derek Chan for the assistance with all the theoretical calculations presented here. We also thank Prof. Thomas Healy for his encouragement and invaluable advice. This work was supported by the U.S. Department of Energy and the Australian Research Council Advanced Mineral Products Research Centre. C.F.Z. also acknowledges the receipt of a Fulbright fellowship. P.M. is the recipient of an ARC QEII Fellowship.

Supplementary Material Available: Details of the calibration of the AFM cantilevers and a plot of the mass of the tungsten spheres placed on the tip of V-shaped cantilever as a function of the square of the reciprocal resonant frequency of the loaded cantilever (2 pages). This material is contained in many libraries on microfiche, immediately follows this article in the microfilm version of the journal, and can be ordered from the ACS; see any current masthead page for ordering information.